

Structure-Guided Rescaffolding of Selective Antagonists of BCL-X<sub>L</sub>

Michael F. T. Koehler,<sup>\*,†</sup> Philippe Bergeron,<sup>†</sup> Edna F. Choo,<sup>‡</sup> Kevin Lau,<sup>†</sup> Chudi Ndubaku,<sup>†</sup> Danette Dudley,<sup>†</sup> Paul Gibbons,<sup>†</sup> Brad E. Sleebs,<sup>||,⊥</sup> Carl S. Rye,<sup>||,⊥,¶</sup> George Nikolakopoulos,<sup>||,⊥</sup> Chinh Bui,<sup>||,⊥</sup> Sanji Kulasegaram,<sup>||,⊥,∇</sup> Wilhelmus J. A. Kersten,<sup>||,⊥</sup> Brian J. Smith,<sup>||,⊥,◆</sup> Peter E. Czabotar,<sup>||,⊥</sup> Peter M. Colman,<sup>||,⊥</sup> David C. S. Huang,<sup>||,⊥</sup> Jonathan B. Baell,<sup>||,⊥,#</sup> Keith G. Watson,<sup>||,⊥</sup> Lisa Hasvold,<sup>○</sup> Zhi-Fu Tao,<sup>○</sup> Le Wang,<sup>○</sup> Andrew J. Souers,<sup>○</sup> Steven W. Elmore,<sup>○</sup> John A. Flygare,<sup>†</sup> Wayne J. Fairbrother,<sup>§</sup> and Guillaume Lessene<sup>||,⊥</sup>

<sup>†</sup>Departments of Discovery Chemistry, <sup>‡</sup>Drug Metabolism and Pharmacokinetics, and <sup>§</sup>Early Discovery Biochemistry, Genentech, Inc., 1 DNA Way, South San Francisco, California 94080, United States

<sup>||</sup>Walter and Eliza Hall Institute of Medical Research, 1G Royal Parade, Parkville, VIC 3052, Australia

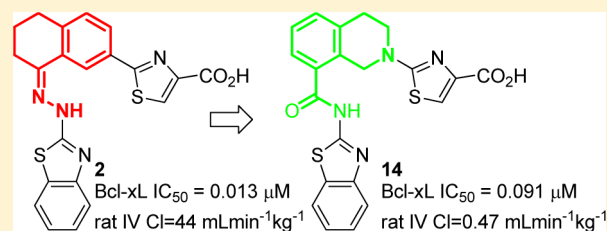
<sup>⊥</sup>Department of Medical Biology, The University of Melbourne, Parkville, Victoria, Australia

<sup>○</sup>AbbVie, Inc., 1 North Waukegan Road, North Chicago, Illinois 60064, United States

**S** Supporting Information

**ABSTRACT:** Because of the promise of BCL-2 antagonists in combating chronic lymphocytic leukemia (CLL) and non-Hodgkin's lymphoma (NHL), interest in additional selective antagonists of antiapoptotic proteins has grown. Beginning with a series of selective, potent BCL-X<sub>L</sub> antagonists containing an undesirable hydrazone functionality, in silico design and X-ray crystallography were utilized to develop alternative scaffolds that retained the selectivity and potency of the starting compounds.

**KEYWORDS:** BCL-X<sub>L</sub>, BCL-2, apoptosis, cancer



Apoptosis, or programmed cell death, is a tightly regulated biological process that is critical for development, for maintenance of cellular homeostasis, and for fighting off infection. The extrinsic<sup>1</sup> apoptotic pathway involves the binding of pro-apoptotic ligands such as Apo2L/TRAIL, TNF, and FasL to specific cell surface receptors. This begins a cascade of events that culminates in the activation of caspase-3, the committed step in apoptosis. The intrinsic<sup>2</sup> apoptotic pathway is initiated when cellular stress stimulates the production of or increased persistence of the pro-apoptotic BH3-only proteins BIM, BID, PUMA, NOXA, BAD, HRK, MBF, and BIK. These proteins interact with the pro-survival proteins BCL-2, BCL-X<sub>L</sub>, BCL-w, MCL-1, and A1 and possibly directly with the apoptotic effector proteins BAX and BAK. Regardless of the interaction they engage in, the pro-apoptotic proteins ultimately induce the permeabilization of the mitochondrial membrane, followed by the activation of caspase-3 and cell death.

Both the intrinsic and extrinsic apoptotic pathways have been targeted for cancer therapy. While research into the extrinsic pathway has focused on Apo2L/TRAIL and its synergies with existing therapy,<sup>3</sup> the focus in the intrinsic pathway has been on the inhibition of pro-survival proteins overexpressed in tumors, including BCL-2, BCL-X<sub>L</sub>, and BCL-w.<sup>4</sup> Navitoclax, an orally available small molecule that potently binds BCL-2, BCL-X<sub>L</sub>, and BCL-w, has already shown promise in human clinical trials.<sup>5–7</sup> Additionally, the inhibitor of apoptosis (IAP) proteins,

which operate immediately downstream of both pathways have been the target of drug development efforts.<sup>8,9</sup>

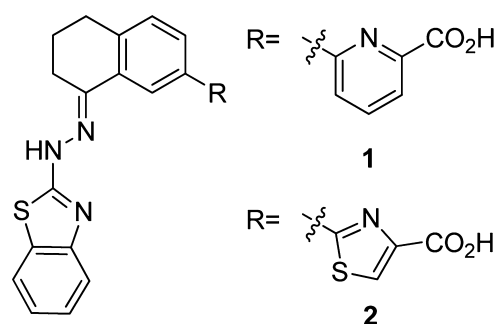
Broad inhibition of the pro-survival proteins carries with it the risk of undesired activities in vivo arising from the fact that these proteins are responsible for maintaining various cell populations under normal conditions. For example, BCL-2 is required for B and T lymphocyte survival,<sup>10</sup> while BCL-X<sub>L</sub> is responsible for platelet survival.<sup>11,12</sup> MCL-1 has been shown to be required for hematopoietic stem cell survival,<sup>13</sup> and BCL-w is essential for developing sperm cells.<sup>14</sup> Narrowly targeting the pro-survival protein responsible for tumor survival or resistance to chemotherapy could thereby allow for a reduced set of side effects, as has been demonstrated by the efficacy without significant thrombocytopenia observed for ABT-199 (GDC-0199), which is a BCL-2 selective inhibitor, in CLL patients.<sup>15</sup> To this end, a series of selective BCL-X<sub>L</sub> antagonists were developed<sup>16</sup> to target solid tumors without concomitant effects on BCL-2 dependent hematopoietic cells.<sup>5,7</sup>

We recently reported compounds 1 and 2 (Figure 1) as potent and selective BCL-X<sub>L</sub> inhibitors. While these represent good lead structures, we were concerned about the presence of a hydrazone in the molecules, as they are known to hydrolyze,

Received: January 22, 2014

Accepted: March 21, 2014

Published: March 21, 2014



|          | Bcl-xL IC <sub>50</sub><br>( $\mu$ M) | Bcl-2 IC <sub>50</sub><br>( $\mu$ M) | rat CL<br>(mLmin <sup>-1</sup> kg <sup>-1</sup> ) | rat F% |
|----------|---------------------------------------|--------------------------------------|---|--------|
| <b>1</b> | 0.020                                 | >10                                  | 9.6   | 8      |
| <b>2</b> | 0.013                                 | 5                                    | 44  | 4      |

**Figure 1.** BCL-X<sub>L</sub> antagonists **1** and **2** incorporating a hydrazone linker between the benzothiazole and bicyclic core. Rat PK data represents an average of three animals dosed at 1 mg/kg IV or 5 mg/kg PO.

potentially releasing a toxic 2-hydrazinylbenzothiazole upon exposure to water. Indeed, when compound **1** was dosed intravenously in rats, the 3,4-dihydronaphthalene-1-one expected from hydrolysis of the parent hydrazone was observed at approximately 1% of the level of **1**, implying the release of 2-hydrazinyl benzothiazole.

In addition to our concerns about the presence of a potential toxicophore, we were concerned about the generally poor pharmacokinetic (PK) properties of these molecules, as they suffered from high clearance, low oral bioavailability, or both in rats. We sought to address these issues through replacement of the hydrazone with a hydrolytically stable linkage while preserving the other favorable attributes of the molecules.

The known structure (PDB: 3ZLN) of compound **1** in complex with BCL-X<sub>L</sub> (Figure 2) was used as a guide for our designs. Our first consideration was the observed enlargement of the hydrophobic P2 pocket upon ligand binding, which appears to be an induced fit to accommodate the benzothiazole.

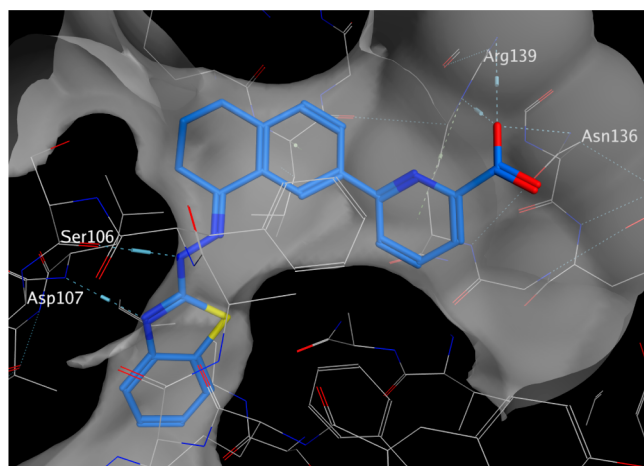


**Figure 2.** Interactions of compound **1** with BCL-X<sub>L</sub> observed in a 2.3 Å resolution crystal structure (PDB: 3ZLN). The surface displayed is one van der Waal's radius above the analytic Connolly surface of the protein. Hydrogen bonds are indicated by dashed lines.

There is little space for the addition of functionality in either the P2 pocket or in the hydrophobic groove containing the tetrahydronaphthalene core. In our initial designs, we therefore attempted to preserve both the hydrophobic nature of the molecules as well as to mimic the overall shape of compounds **1** and **2** as closely as possible.

Our previous structures and structure–activity relationship (SAR) experience made it clear that we needed to preserve the multiple contacts made by the polar atoms in the picolinic acid with Arg139 of BCL-X<sub>L</sub>. Similarly, it was clear that the hydrazone nitrogen closest to the benzothiazole served as a hydrogen bond donor to the backbone carbonyl of Ser106 and that the benzothiazole nitrogen accepts a hydrogen bond from the main chain NH of Asp107. We therefore incorporated the picolinic acid as well as a hydrogen bond donor/acceptor pair of the 2-amino benzothiazole ring into our designs.

The initial complement of analogues prepared included the replacement of the hydrazone with an amine, an amide, and a urea while varying the degree of saturation in the core naphthalene/tetrahydronaphthalene to afford compounds **3–7** (Figure 3). In preparing compounds **5** and **6**, we did not attempt to control the stereochemistry, although docking experiments indicate that the *R* enantiomer should be preferred in both cases. The enantiomers were separated following synthesis and assayed individually.

Following their synthesis (described in Schemes S1–S4, Supporting Information), compounds **3–7** were examined for their ability to inhibit binding of a 26-mer BIMBH3 peptide to BCL-X<sub>L</sub>, as described previously.<sup>16</sup> The naphthalene amide **4** and tetrahydroquinoline urea **7** were the strongest inhibitors of the group, but were 36- to 50-fold weaker binders, respectively, than hydrazone **1**. Although the compounds lacking the hydrazone functionality still retained measurable binding to BCL-X<sub>L</sub>, refinement of our designs was clearly necessary in order to attain biologically relevant levels of inhibition.

Docking experiments with higher affinity ligands **5b** and **7** pointed to two new unfavorable interactions introduced in the carbonyl-containing compounds. One straightforward explanation for the loss of affinity was the desolvation penalty incurred by the introduction of a hydrophilic carbonyl group into the highly lipophilic environment of the binding pocket formed by the side chains from Phe97, Phe105, and Ala142. More subtly, our docking experiments indicated that **4**, **6**, and **7** might not be able to align their hydrogen bond donating NH optimally toward Ser106 as this would force the carbonyl oxygen into an unfavorable steric interaction with the adjacent aryl ring.

As our most potent new analogues all included the carbonyl oxygen proposed to be producing these unfavorable interactions, we set out to mitigate these effects. We initially attempted to relieve the steric clash between the carbonyl and the proton at the 1-position of the naphthalene through exploration of [5,6]-fused heterocycles. Accordingly, we prepared analogues **8–10** (Schemes S5–S7, Supporting Information) and evaluated their ability to bind to BCL-X<sub>L</sub> as before.

Unfortunately, none of the compounds showed improved affinity for the target. Although **8** was predicted to have an improved ability to engage Ser106, the inclusion of new polar functionality into the biaryl ring system may have introduced additional detrimental interactions. A measure of polarity change can be seen in the increased topological polar surface area (TPSA) of imidazopyridine **8** (109 Å<sup>2</sup>) relative to **6** (92

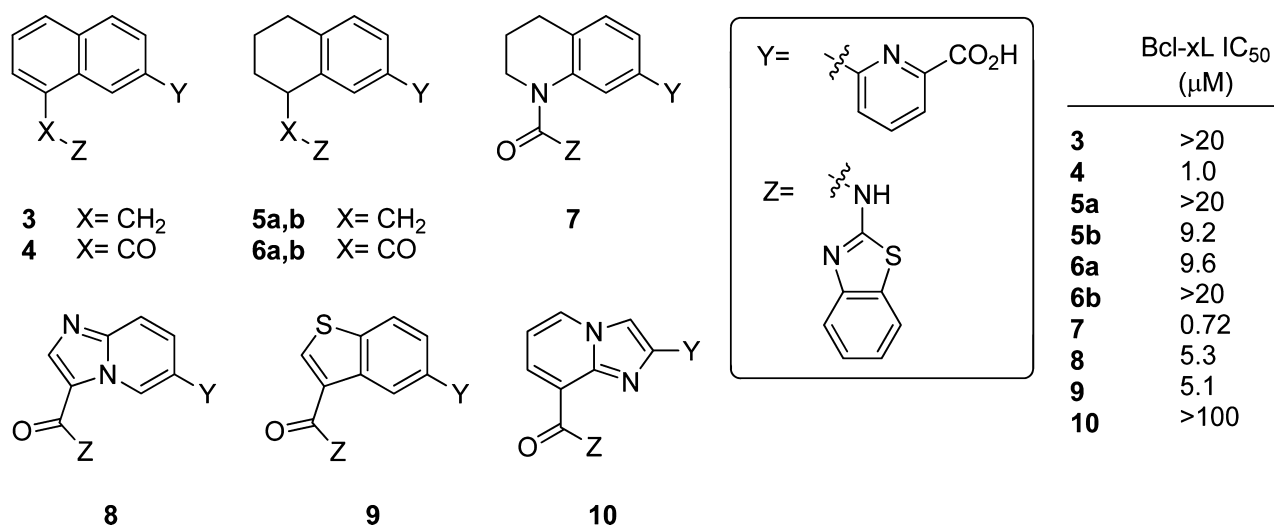


**Figure 3.** Initially prepared analogues of **1** along with their inhibitory activity toward BCL-X<sub>L</sub>. Compounds **5** and **6** were assayed as single enantiomers. Their absolute configuration was not determined.

Å<sup>2</sup>). Compound **9**, whose benzothiophene ring is very similar in size and geometry to the naphthalene amide **4**, binds 5-fold more weakly for reasons that are not clear. The second imidazopyridine, **10**, may be able to interact more beneficially in the region of the benzothiazole, but docking experiments point to the altered spatial relationship of the key polar binding interactions of the amino benzothiazole and the picolinate as the reason for its lack of activity. It is also possible that an intramolecular hydrogen bond between the amide NH and the imidazopyridine leaves the amide unable to interact with Ser106.

Having failed to improve upon the amides through altered ring size, we returned to urea **7**, the highest affinity binder in the first set of ligands prepared. This compound demonstrates that the inclusion of a saturated ring can preserve the key binding interactions. Interchanging the position of the saturated and unsaturated rings was proposed in order to allow the amide carbonyl oxygen additional flexibility, enabling the amide NH to optimally engage Ser106. When synthetic considerations were taken into account, tetrahydroisoquinolines **13** and **14** were selected as our next targets.

The starting point for synthesis of these compounds was the Boc-protected tetrahydroisoquinoline **11**, which was coupled to 2-aminobenzothiazole using standard peptide coupling conditions. Removal of the Boc group gave **12**, which could be coupled to *t*-butyl-6-fluoropicolinate or to methyl 2-chlorothiazole-4-carboxylate to give compounds **13** and **14**, respectively, following hydrolysis of the ester. When evaluated for their ability to bind BCL-X<sub>L</sub>, these compounds were found to exhibit significantly improved affinity (Figure 4). Compound **14** is particularly potent and exhibits an IC<sub>50</sub> value only 7-fold higher than that of the hydrazone **2**, the starting point for our rescaffolding experiments.

Having minimized the loss of potency resulting from the rescaffolding effort, we next sought to improve the binding affinity of our molecules through extension into a known, adjacent binding region on the protein. Multiple structures, determined both as NMR solution structures<sup>17,18</sup> and as X-ray cocrystal structures,<sup>16,19</sup> have shown that there exists a lipophilic P4 pocket in the region immediately adjacent to the picolinate region of our molecules. We therefore sought to extend the tetrahydroisoquinoline analogues from the 3-

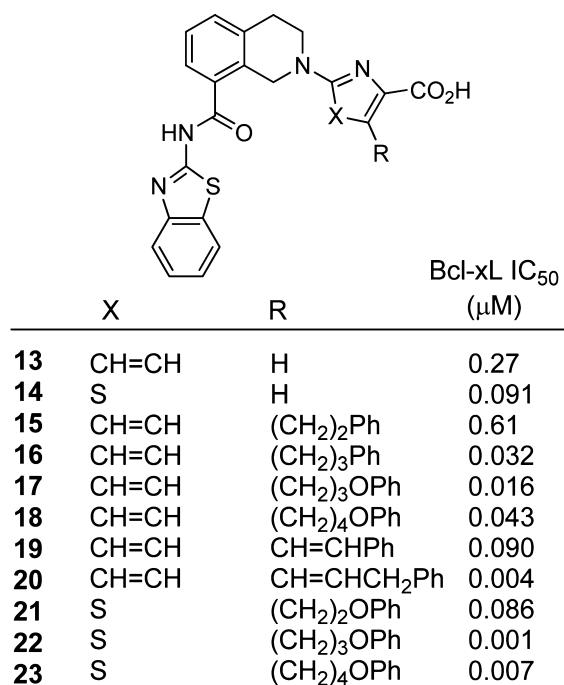


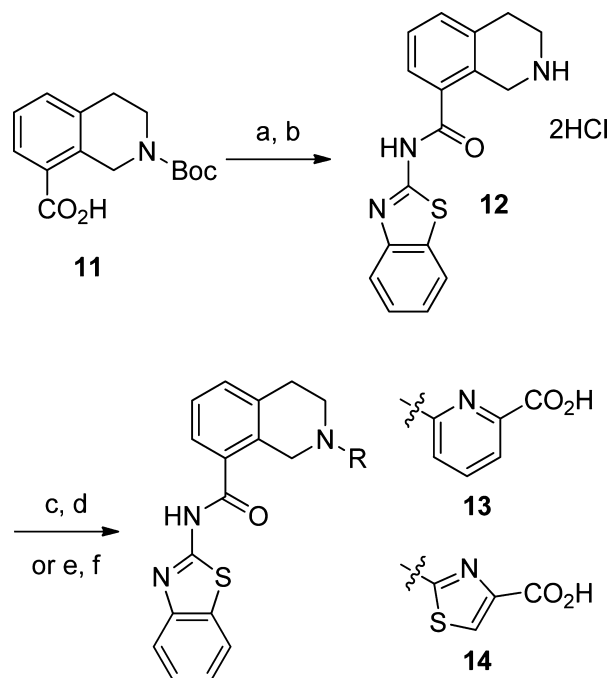
**Figure 4.** Tetrahydroisoquinolines with and without extensions into the P4 pocket along with AlphaScreen measured IC<sub>50</sub> values for BCL-X<sub>L</sub>. Compounds **19** and **20** were synthesized as the trans isomer.

position of the picolinate **13** and from the 5-position of the thiazole **14** into this pocket.

Following their synthesis (described in Schemes S9–S16, Supporting Information), compounds **15–23** provided a clear picture of the optimal length and flexibility required to take advantage of the P4 pocket. Beginning from the picolinate, compounds **15–20** showed improvements in affinity as the number of heavy atoms included before the phenyl was increased from two to four. Adding a further methylene reduced the potency greater than 2-fold, indicating that the entropic cost of organizing the longer carbon chain and/or a reduced enthalpy of binding due to inappropriate positioning of the P4 binding element resulted in a reduction in affinity for the target.

The potency of these compounds (Scheme 1) was further improved through the incorporation of a trans double bond

Scheme 1. Synthesis of Tetrahydroisoquinolines 13 and 14<sup>a</sup>



<sup>a</sup>Reagents and conditions: (a) benzo [*d*]thiazol-2-amine, EDCI, DMAP, DCM; (b) 2 N HCl/Et<sub>2</sub>O, DCM; (c) *t*-butyl 6-fluoropyridine-2-carboxylate, Cs<sub>2</sub>CO<sub>3</sub>, DMA, sieves, 100 °C, 29%; (d) HCl, EtOH, H<sub>2</sub>O, 67%; (e) methyl 2-chlorothiazole-4-carboxylate, Cs<sub>2</sub>CO<sub>3</sub>, DMA, 50 °C, 67%; (f) 2 N NaOH, THF/MeOH, 50 °C.

into the carbon chain, reducing the number of degrees of freedom available to the spacer and thereby lowering the entropy of binding. This reduction led to a nearly 7-fold improvement in the IC<sub>50</sub> of the two-atom spacer and to an 8-fold improvement in the IC<sub>50</sub> of the three-atom spacer. Parallel results were obtained for the thiazole containing compounds 14 and 21–23. Inclusion of the optimal four-atom spacer and a phenyl ring produced the 1 nM inhibitor 22; increasing the length of the spacer to five atoms led to a 7-fold increase in the measured IC<sub>50</sub>, again suggesting that a four atom linker is optimal.

Key compounds 13, 14, and 22 were subsequently examined for their ability to induce apoptosis in an engineered cell line. All three compounds are highly selective for BCL-X<sub>L</sub> over the closely related pro-survival proteins BCL-2, BCL-w, and Mcl-1. As previously described,<sup>16</sup> mouse embryonic fibroblast (MEF) cells were engineered to be MCL-1 deficient (*mcl-1*<sup>-/-</sup>) such

that inhibition of the lone survival factor BCL-X<sub>L</sub> induces apoptosis. Treatment of these cells with compounds 1 and 2 produces IC<sub>50</sub> values of 0.29 and 0.26 μM, respectively. As would be expected from a compound with 10-fold reduced affinity in the Alpha-Screen assay, compound 13 has an IC<sub>50</sub> value of 2.4 μM (Table 1). Compound 22 has a 14 nM IC<sub>50</sub> in this assay and is therefore significantly more active than the compounds from which it was derived.

The selectivity of our compounds was assessed through surface plasmon resonance binding experiments. Curiously, although our core compounds 13 and 14 are highly selective for BCL-X<sub>L</sub> over other pro-survival proteins, compound 22 bound BCL-w unexpectedly well with a K<sub>d</sub> of 62 nM. This still results in greater than 12-fold selectivity due to its increased affinity for BCL-X<sub>L</sub>, but additional SAR studies of the P4 binding group and its linker will be required to improve selectivity against BCL-w.

We next characterized the pharmacokinetics of the rescaffolded molecules in rats. We were gratified to find that both compounds 13 and 14 exhibited low clearance and long half-lives when dosed intravenously at 1 mg/kg (Table 1). Compound 13 was found to have excellent oral bioavailability (*F*%) with compound 14 being significantly lower. When the phenoxy alkyl tail was appended to the scaffold, clearance was increased more than 10-fold to 7.4 mL min<sup>-1</sup> kg<sup>-1</sup> and oral bioavailability was reduced nearly to zero. However, the enhanced stability of the core in vivo gave us confidence that these parameters could be improved upon through further optimization of the portion of the molecule accessing the P4 pocket, initially by reducing its high clogP and multiple metabolic soft spots.

To further our understanding of the interactions that we had sought to optimize, the structure of compound 20 was determined to 2.35 Å resolution in complex with BCL-X<sub>L</sub> (Figure 5). This structure confirmed that our molecules were indeed binding in a fashion very similar to hydrazone 1. The hydrogen bonds from the 2-aminobenzothiazole to Ser106 and Leu108 are very similar to those observed in the structure of 1 bound to BCL-X<sub>L</sub>. The tetrahydroisoquinoline core packs against Leu130 and Phe105 much as 1 does, and the interactions of Asn136 and Arg139 with the picolinic acid carbonyl group are preserved.

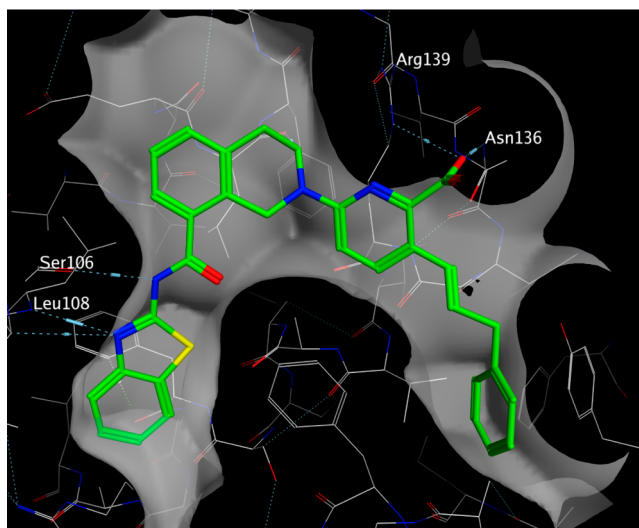
In addition to the expected interactions, we were able to observe for the first time the interactions of our ligand with the P4 pocket. The pocket is flanked by aromatic and hydrophobic side chains including Phe97, Tyr101, Val141, and Tyr195, which all make van der Waals' contacts with the phenyl ring. The only significant residue shift was seen for Tyr101, which rotates and shifts away from the P4 pocket's center to allow insertion of the phenyl ring. We were intrigued to observe the position of Glu96 along the vectors extending from the 3- or 4-

Table 1. Selectivity, Cellular, and Pharmacokinetic Data Obtained in Rat for Compounds 13, 14, and 22<sup>a</sup>

| EC <sub>50</sub> <i>Mcl-1</i> <sup>-/-</sup> MEF, 1% FBS (μM) | rat PK  |        |       |       |  |                        |                      |              |     |  |
|---|---|--------|-------|-------|--|------------------------|----------------------|--------------|-----|--|
|   | surface plasmon resonance K <sub>d</sub> (μM) |        |       |       | iv (1 mg/kg)   |                        |                      | po (5 mg/kg) |     |  |
|   | BCL-xL  | BCL-2  | BCL-w | Mcl-1 | CL <sub>p</sub> (mL min <sup>-1</sup> kg <sup>-1</sup> ) | V <sub>ss</sub> (L/kg) | t <sub>1/2</sub> (h) | <i>F</i> %   |     |  |
| 13  | 2.4   | 0.038  | >20   | >20   | >20  | 0.20                   | 0.12                 | 8.3          | 60  |  |
| 14  | n/d   | 0.010  | 9.2   | 7.8   | >20  | 0.47                   | 0.16                 | 6.0          | 16  |  |
| 22  | 0.014   | <0.005 | 4.4   | 0.062 | 14.4   | 7.4                    | 0.31                 | 3.6          | 0.2 |  |

<sup>a</sup>Selectivity was measured using a surface plasmon resonance competition assay (*n* = 3). n/d indicates that the compound was not evaluated in a given assay.





**Figure 5.** Interactions of compound **20** with BCL- $X_L$  observed in a 2.35 Å resolution crystal structure. The surface displayed is one van der Waal's radius above the analytic Connolly surface of the protein. Hydrogen bonds are indicated by dashed lines.

position of the phenyl ring, which suggested additional polar contacts that might be accessible via the addition of functional groups to this scaffold.

In summary, application of a combination of docking studies and rational design enabled the conversion of an undesirable hydrazone-based core to amide and urea-based ligands, which preserve many of the binding interactions and nearly all of the affinity of the parent compounds. As exemplified by compounds **13** and **14**, these rescaffolded molecules exhibit significantly better clearance and oral bioavailability than the parent hydrazones **1** and **2** when dosed in rats.

Building on this more desirable core, both the biochemical and cellular affinity of the rescaffolded molecules for BCL- $X_L$  was increased through incorporation of aryl rings at the 3-position of the picolinic acid or the corresponding 5-position of the thiazole ring. These were demonstrated to be interacting as designed with the lipophilic P4 pocket and increased the affinity of our compounds for BCL- $X_L$  to single-digit nanomolar levels in the best case. This improved affinity was also reflected in activity in our *mcl-1*<sup>-/-</sup> MEF cell line, with the most potent molecule exhibiting an IC<sub>50</sub> of 14 nM, a nearly 20-fold improvement in cellular potency. Having determined the structure of **20** in complex with BCL- $X_L$ , we confirmed our hypotheses about the binding mode of these molecules and observed additional possibilities for refinement, which will be reported in due course.

## ■ ASSOCIATED CONTENT

### Ⓢ Supporting Information

Synthetic schemes, procedures, and analytical data describing the preparation of compounds **3**–**23** as well as experimental procedures for determining IC<sub>50</sub> and EC<sub>50</sub> values and PK. This material is available free of charge via the Internet at <http://pubs.acs.org>.

## ■ AUTHOR INFORMATION

### Corresponding Author

\*(M.F.T.K.) Phone: 650-225-8135. Fax: 650-467-8922. E-mail: [mkoehler@gene.com](mailto:mkoehler@gene.com).

## Present Addresses

<sup>∇</sup>(S.K.) Monash University, Chemistry Department, Clayton, VIC 3800, Australia.

<sup>#</sup>(J.B.B.) Peter MacCallum Cancer Centre, Melbourne, VIC 3006, Australia.

<sup>‡</sup>(C.S.R.) The Institute of Cancer Research, Belmont, Sutton, Surrey, SM2 5NG, U.K.

<sup>◆</sup>(B.J.S.) La Trobe Institute for Molecular Science, La Trobe University, VIC 3086 Australia.

## Funding

Part of this work was supported by fellowships and grants from the Australian Research Council (fellowship to P.E.C.), the National Health and Medical Research Council (NHMRC, fellowships to J.M.A., J.B.B., P.M.C., and D.C.S.H.; development grant 305536 and program grants 257502, 461221, and 1016701), the Leukemia and Lymphoma Society (specialized center of research grant nos. 7015 and 7413), the Cancer Council of Victoria (fellowship to P.M.C.; grant-in-aid 461239), and the Australian Cancer Research Foundation. Infrastructure support from the NHMRC Independent Research Institutes Infrastructure Support Scheme grant no. 361646 and a Victorian State Government OIS grant are gratefully acknowledged.

## Notes

The authors declare no competing financial interest.

## ■ ACKNOWLEDGMENTS

We thank members of the DMPK and purification groups within Genentech Small Molecule Drug Discovery for analytical support and Ahmad Wardak and Geoff Thompson for technical support.

## ■ REFERENCES

- (1) Gonzalez, F.; Ashkenazi, A. New insights into apoptosis signaling by Apo2L/TRAIL. *Oncogene* **2010**, *29*, 4752–4765.
- (2) Czabotar, P. E.; Lessene, G. Bcl-2 family proteins as therapeutic targets. *Curr. Pharm. Des.* **2010**, *16*, 3132–3148.
- (3) Sayers, T. J. Targeting the extrinsic apoptosis signaling pathway for cancer therapy. *Cancer Immunol. Immunother.* **2011**, *60*, 1173–1180.
- (4) Lessene, G.; Czabotar, P. E.; Colman, P. M. BCL-2 family antagonists for cancer therapy. *Nat. Rev. Drug Discovery* **2008**, *7*, 989–1000.
- (5) Rudin, C. M.; Hann, C. L.; Garon, E. B.; Ribeiro de Oliveira, M.; Bonomi, P. D.; Camidge, D. R.; Chu, Q.; Giaccone, G.; Khaira, D.; Ramalingam, S. S.; Ranson, M. R.; Dive, C.; McKeegan, E. M.; Chyla, B. J.; Dowell, B. L.; Chakravarty, A.; Nolan, C. E.; Rudersdorf, N.; Busman, T. A.; Mabry, M. H.; Krivoshik, A. P.; Humerickhouse, R. A.; Shapiro, G. I.; Gandhi, L. Phase II study of single-agent navitoclax (ABT-263) and biomarker correlates in patients with relapsed small cell lung cancer. *Clin. Cancer Res.* **2012**, *18*, 3163–3169.
- (6) Wilson, W. H.; O'Connor, O. A.; Czuczman, M. S.; LaCasce, A. S.; Gerecitano, J. F.; Leonard, J. P.; Tulpule, A.; Dunleavy, K.; Xiong, H.; Chiu, Y.-L.; Cui, Y.; Busman, T.; Elmore, S. W.; Rosenberg, S. H.; Krivoshik, A. P.; Enschede, S. H.; Humerickhouse, R. A. Navitoclax, a targeted high-affinity inhibitor of BCL-2, in lymphoid malignancies: a phase 1 dose-escalation study of safety, pharmacokinetics, pharmacodynamics, and antitumour activity. *Lancet Oncol.* **2010**, *11*, 1149–1159.
- (7) Roberts, A. W.; Seymour, J. F.; Brown, J. R.; Wierda, W. G.; Kipps, T. J.; Khaw, S. L.; Carney, D. A.; He, S. Z.; Huang, D. C. S.; Xiong, H.; Cui, Y.; Busman, T. A.; McKeegan, E. M.; Krivoshik, A. P.; Enschede, S. H.; Humerickhouse, R. Substantial susceptibility of chronic lymphocytic leukemia to BCL2 inhibition: results of a phase I

study of navitoclax in patients with relapsed or refractory disease. *J. Clin. Oncol.* **2012**, *30*, 488–496.

(8) Deshayes, K.; Murray, J.; Vucic, D. The development of small-molecule IAP antagonists for the treatment of cancer. *Top. Med. Chem.* **2012**, *8*, 81–104.

(9) Flygare, J. A.; Fairbrother, W. J. Small-molecule pan-IAP antagonists: a patent review. *Expert Opin. Ther. Pat.* **2010**, *20*, 251–267.

(10) Veis, D. J.; Sorenson, C. M.; Shutter, J. R.; Korsmeyer, S. J. Bcl-2-deficient mice demonstrate fulminant lymphoid apoptosis, polycystic kidneys, and hypopigmented hair. *Cell* **1993**, *75*, 229–240.

(11) Zhang, H.; Nimmer, P. M.; Tahir, S. K.; Chen, J.; Fryer, R. M.; Hahn, K. R.; Cielek, L. A.; Morgan, S. J.; Nasarre, M. C.; Nelson, R.; Preusser, L. C.; Reinhart, G. A.; Smith, M. L.; Rosenberg, S. H.; Elmore, S. W.; Tse, C. Bcl-2 family proteins are essential for platelet survival. *Cell Death Differ.* **2007**, *14*, 943–951.

(12) Mason, K. D.; Carpinelli, M. R.; Fletcher, J. I.; Collinge, J. E.; Hilton, A. A.; Ellis, S.; Kelly, P. N.; Ekert, P. G.; Metcalf, D.; Roberts, A. W.; Huang, D. C. S.; Kile, B. T. Programmed anuclear cell death delimits platelet life span. *Cell* **2007**, *128*, 1173–1186.

(13) Rinckenberger, J. L.; Horning, S.; Klocke, B.; Roth, K.; Korsmeyer, S. J. Mcl-1 deficiency results in peri-implantation embryonic lethality. *Genes Dev.* **2000**, *14*, 23–27.

(14) Ross, A. J.; Waymire, K. G.; Moss, J. E.; Parlow, A. F.; Skinner, M. K.; Russell, L. D.; MacGregor, G. R. Testicular degeneration in Bclw-deficient mice. *Nat. Genet.* **1998**, *18*, 251–256.

(15) Souers, A. J.; Levenson, J. D.; Boghaert, E. R.; Ackler, S. L.; Catron, N. D.; Chen, J.; Dayton, B. D.; Ding, H.; Enschede, S. H.; Fairbrother, W. J.; Huang, D. C. S.; Hymowitz, S. G.; Jin, S.; Khaw, S. L.; Kovar, P. J.; Lam, L. T.; Lee, J.; Maecker, H. L.; Marsh, K. C.; Mason, K. D.; Mitten, M. J.; Nimmer, P. M.; Oleksijew, A.; Park, C. H.; Park, C.-M.; Phillips, D. C.; Roberts, A. W.; Sampath, D.; Seymour, J. F.; Smith, M. L.; Sullivan, G. M.; Tahir, S. K.; Tse, C.; Wendt, M. D.; Xiao, Y.; Xue, J. C.; Zhang, H.; Humerickhouse, R. A.; Rosenberg, S. H.; Elmore, S. W. ABT-199, a potent and selective BCL-2 inhibitor, achieves antitumor activity while sparing platelets. *Nat. Med.* **2013**, *19*, 202–208.

(16) Lessene, G.; Czabotar, P. E.; Sleebs, B. E.; Zobel, K.; Lowes, K. N.; Adams, J. M.; Baell, J. B.; Colman, P. M.; Deshayes, K.; Fairbrother, W. J.; Flygare, J. A.; Gibbons, P.; Kersten, W. J. A.; Kulasegaram, S.; Moss, R. M.; Parisot, J. P.; Smith, B. J.; Street, I. P.; Yang, H.; Huang, D. C. S.; Watson, K. G. Structure-guided design of a selective BCL-XL inhibitor. *Nat. Chem. Biol.* **2013**, *9*, 390–397.

(17) Petros, A. M.; Dinges, J.; Augeri, D. J.; Baumeister, S. A.; Betebenner, D. A.; Bures, M. G.; Elmore, S. W.; Hajduk, P. J.; Joseph, M. K.; Landis, S. K.; Nettlesheim, D. G.; Rosenberg, S. H.; Shen, W.; Thomas, S.; Wang, X.; Zanze, I.; Zhang, H.; Fesik, S. W. Discovery of a potent inhibitor of the antiapoptotic protein Bcl-xL from NMR and parallel synthesis. *J. Med. Chem.* **2006**, *49*, 656–663.

(18) Bruncko, M.; Oost, T. K.; Belli, B. A.; Ding, H.; Joseph, M. K.; Kunzer, A.; Martineau, D.; McClellan, W. J.; Mitten, M.; Ng, S.-C.; Nimmer, P. M.; Oltersdorf, T.; Park, C.-M.; Petros, A. M.; Shoemaker, A. R.; Song, X.; Wang, X.; Wendt, M. D.; Zhang, H.; Fesik, S. W.; Rosenberg, S. H.; Elmore, S. W. Studies leading to potent, dual inhibitors of Bcl-2 and Bcl-xL. *J. Med. Chem.* **2007**, *50*, 641–662.

(19) Lee, E. F.; Czabotar, P. E.; Smith, B. J.; Deshayes, K.; Zobel, K.; Colman, P. M.; Fairlie, W. D. Crystal structure of ABT-737 complexed with Bcl-xL: implications for selectivity of antagonists of the Bcl-2 family. *Cell Death Differ.* **2007**, *14*, 1711–1713.